

## Experimental study on the effect of drop size in rain erosion test and on lifetime prediction of wind turbine blades

Jakob Ilsted Bech<sup>a,\*</sup>, Nicolai Frost-Jensen Johansen<sup>a</sup>, Martin Bonde Madsen<sup>b</sup>,  
Ásta Hannesdóttir<sup>a</sup>, Charlotte Bay Hasager<sup>a</sup>

<sup>a</sup> Technical University of Denmark, Department of Wind and Energy Systems, Frederiksbergvej 399, 4000, Roskilde, Denmark

<sup>b</sup> R&D Test Systems A/S, Kystvejen 100, 5530, Munkebo, Denmark

### ARTICLE INFO

#### Keywords:

Rain erosion test  
Impingement to end of incubation  
Drop-size dependency  
Wind turbine blade coating  
Site specific lifetime modelling  
Phenomenological damage model

### ABSTRACT

Rain erosion of turbine blades causes loss of production and expensive repairs in the wind energy sector. There is a common consensus, that the size of impacting rain drops has a governing effect on the added damage. However, the literature lacks systematic experimental studies on the topic. In the present paper the effects of drop sizes in Rain Erosion Tests (RET) are studied for a commercial polyurethane based top coat applied to glass fiber-epoxy specimens. The tests are conducted applying a whirling arm RET at impact velocities ranging from 90 to 150 m/s and with four different rain field setups generating mean droplet diameters of 0.76 mm, 1.90 mm, 2.38 mm and 3.50 mm respectively. The time to damage at the end of incubation is determined by inspection of photographs captured inline at regular intervals through the test.

Data sets of time to damage as function of local rotor velocity are extracted for each of the four different rain fields. From this data VQ curves (V for Velocity, Q for Quantity) are presented for different representations of quantity, namely specific impacts (DNV GL), specific impacts (ASTM) and accumulated impingement. The slope of the velocity-impingement (VH) curves vary with drop size.

We propose a drop size dependent empirical model for impingement ( $H$ ) to damage as function of impact velocity ( $v$ ),  $H(v) = cv^{-m}$ , where the scale parameter  $m$  and the shift parameter  $c$  are functions of the drop size.

The drop size-dependent impingement model is then applied for computing the expected leading edge lifetime of a virtual 15 MW IEA reference turbine at 18 different meteorological stations in Northern Europe based on 10-min time series of rain intensity and wind speeds observed during several years. The drop size dependent model predicted on average 2.35 times longer lifetime compared to models based on the standard 2.38 mm drop size. Comparing the sites, the model shows a factor 3 variation of added damage per meter of accumulated rain between sites because of differences in concurrent wind during the rain events.

### 1. Introduction

Rain erosion of wind turbine blades is a prominent challenge for the wind energy industry [1,2]. When erosion occurs, it causes roughening of the blade surfaces, leading to reduction in aerodynamic efficiency, and potentially losses in annual energy production [3,4]. Wind turbine blades may need repeated repairs during a lifetime, and blade repair costs are high, particularly offshore, due to logistics [5]. Consequently, erosion needs to be considered when planning and operating wind parks, designing wind turbines and developing blade coatings and protection systems. The prevalence and progression of leading edge erosion at wind turbines in operation depend on rotor tip speeds, leading edge

materials, rain and wind, and other environmental parameters. Erosion shows variability between sites, not only because of different turbines and blade coatings, but also because of different meteorological conditions, where concurrent values of precipitation and wind speed are the main meteorological drivers [6,7]. The drop size distribution of the impinging rain also play a significant role. The drop size distribution varies with rain intensity, but also with type of rain, temperature and humidity [8].

The correlation between drop size of impinging rain and added damage to coated composites is thus of great importance for modelling of rain erosion. Several models take into account the effect of drop size on impingement damage [9–12]. However, no experimental validation

\* Corresponding author.

E-mail address: [jakb@dtu.dk](mailto:jakb@dtu.dk) (J.I. Bech).

and studies are found in literature.

In the current work, the whirling arm rain erosion test [13], is used to study the effect of drop size and impact speed on erosion damage. A new empirical drop size dependent impingement model is proposed and used to predict the expected blade lifetime for a virtual IEA Wind 15 MW reference turbine [14] at 18 North European sites using site-specific rain intensity and wind speed time series.

The paper is structured as follows. Section 2 contains a description of the experimental methods and materials, the analysis of tests data, and the meteorological data and wind turbine characteristics used in the lifetime predictions. Section 3 describes different representations of impinging rain and resulting damage and analysis steps. Results are presented in Section 4, followed by Discussion in Section 5, Limitation and proposals for further research in section 6 and conclusion in section 7.

## 2. Experiment and data description

### 2.1. Rain erosion test

The rain erosion tests are conducted with a rain erosion tester (RET) from the company R&D Test Systems A/S. This RET, Fig. 1, has a 3-bladed rotor with one test specimen per blade and a rotor diameter of approximately 2.5 m. The RET is capable of rotational speeds ranging from 500 to 1386 RPM, producing tip speeds from 63 to 172 m/s, and up to 1790 RPM/224 m/s in the aerospace configuration. The rain field is generated from an array of drop dispensing needles. The flow of water is adjustable between 60 and 120 l/h. The drop size depends on the needle size and water flow rate. Standard flow rates are determined as the flow rates giving the narrowest distribution of drop size.

In the experimental set up three needle types were used with standard flow rates. Needles G20 provide uniform droplet sizes around 3.0–3.5 mm diameter at flow rate 120 l/h, G27 around 2.0–2.5 mm droplets at 60 l/h and G30 around 1.4–1.9 mm mm droplets at 85 l/h. The standard flow is low such that the droplet size is mainly controlled by force equilibrium of gravitational force and surface tension when the hanging droplet forms and eventually releases itself. The gravitational acceleration and the vertical distance from the needle array determine the fall velocity of the drops when they enter the rotor plane. Furthermore, G27 needles were also used in spray mode with a higher flow rate of 105 l/h. In this case the water is forced out in a stream that breaks up

into smaller droplets with greater variation in droplet sizes and fall velocities. The rain erosion tests were conducted at three different rotor speeds, 800, 996 and 1193 rpm for each of the four nozzle and flow configurations, resulting in a total of 12 rain erosion test runs. Images, Fig. 4 a), were captured automatically throughout the test at set intervals from 10 to 60 min. The images are later analyzed to identify the erosion damage as function of time and position on the specimens.

Details on the use of the RET are covered in the DNV GL recommended practices 0171 and 0573 [13,15]. A sketch of the R&D RET is shown in Fig. 1. The rotor with the three blades can be seen in the center of the tester. The array of drop dispensing needles are placed at uniform distance on radial manifolds above the rotor.

### 2.2. Droplet sizes and fall velocity verification using disdrometer

The droplet sizes and droplet fall velocity in the RET were measured using a Parsivel<sup>2</sup> disdrometer during rotor standstill for three of the four rain fields. For the fourth drop size, drop count and volume measurements were done to determine the average drop size. The fall velocity of a drop as function of the falling height can be calculated applying a model for the acceleration of droplets in the gravity field as detailed in Refs. [13,16].

### 2.3. Specimen description

The Glass Fiber Reinforced Polymer (GFRP) specimens were made by infusion of epoxy in a 12-layer glass fiber bi-axial layup. A putty layer of 850–950 µm and a top coat of 100–150 µm were applied manually. The top coat is a commercial polyurethane (PU) based coating with good erosion resistance [16]. A cross section of the top coat, putty layer and outermost glass fiber bundles is shown in Fig. 2.

Fig. 3 shows a close-up of progressed erosion on two tested RET specimens. Where the white topcoat is removed, the light brown pore filler is exposed. Finally the blue epoxy/glass fiber laminate becomes visible. The small droplets form a progressive and distributed progression of the erosion, whereas the large droplets form a more localized damage.

### 2.4. Measuring damage progression

After the test is completed, each image, representing a time slice, is

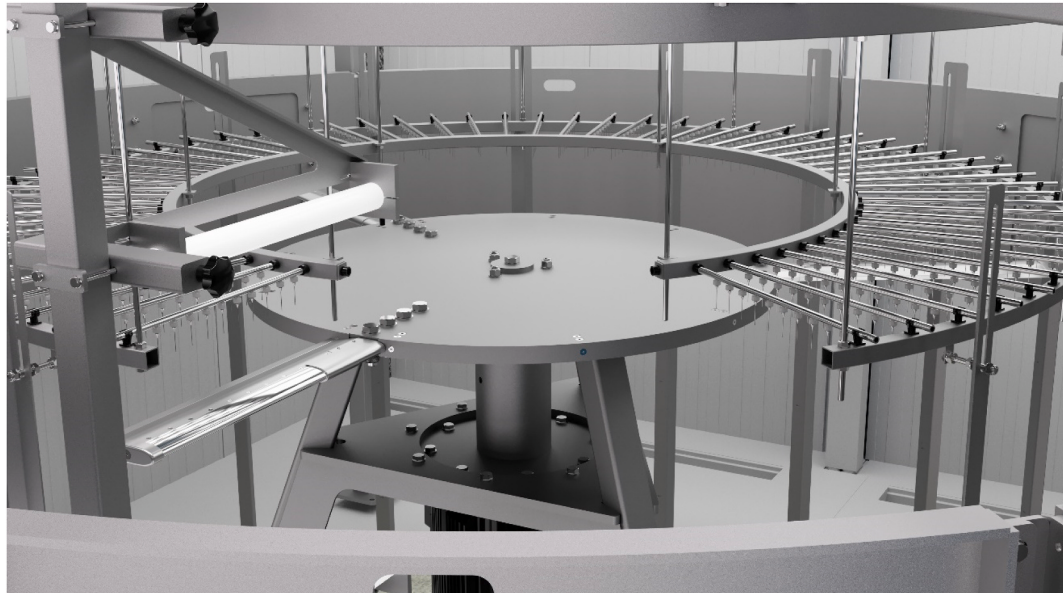
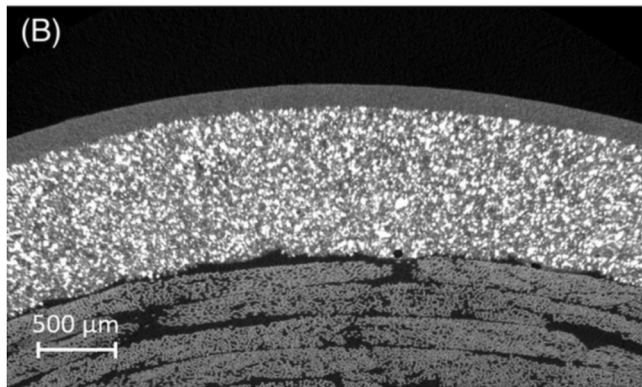


Fig. 1. The rain Erosion Test (RET) unit at R&D.



**Fig. 2.** RET specimen cross-section showing the top coat, putty layer and glass fiber bundles [16].

inspected manually, and new isolated erosion points or surface damages are registered [16]. Fig. 4 a) shows inline photo of an eroded sample, where initial erosion points are marked with circles. At the high speed end to the left, one can see further progressed erosion points. The damage usually initiates near the tip of the specimen, having the highest velocity, and propagates towards the root with lower velocities. The data obtained are radial positions of new damage points as a function time. The correlating number of droplet impacts ( $N$ ) and amount of

impinged water ( $H$ ), for the velocity ( $v$ ) are later computed as described in Section 3.

The data can be fitted to a power law function,

$$N(v) = cv^{-m} \quad (1)$$

where  $N$  is a measure of impinged water, and  $v$  is the local rotor velocity

$$v=r\omega \quad (2)$$

$r$  is the radius and  $\omega$  is the angular velocity of the rotor.

## 2.5. Lifetime calculations

Lifetime calculations are here based on Palmgren-Miner's rule, as suggested by Ref. [17]. The linear summation of damage increments using the Palmgren-Miner rule results in the accumulated damage sum ( $D$ ) given by

$$D = \sum_{i=1}^k \frac{n_i}{N_i} \quad (3)$$

The expected end of incubation and initial failure of the coating is reached when  $D = 1$ . When analyzing RET images, this local end of incubation is determined as the first visible erosion point, as described in section 2.4 and [16]. In Equation (3)  $k$  is the number of bins in a meteorological time series.  $N_i$  is the quantity of impinged water in bin  $i$ .  $N_i$  is the expected impinged water to end of incubation given by eq. (1) at

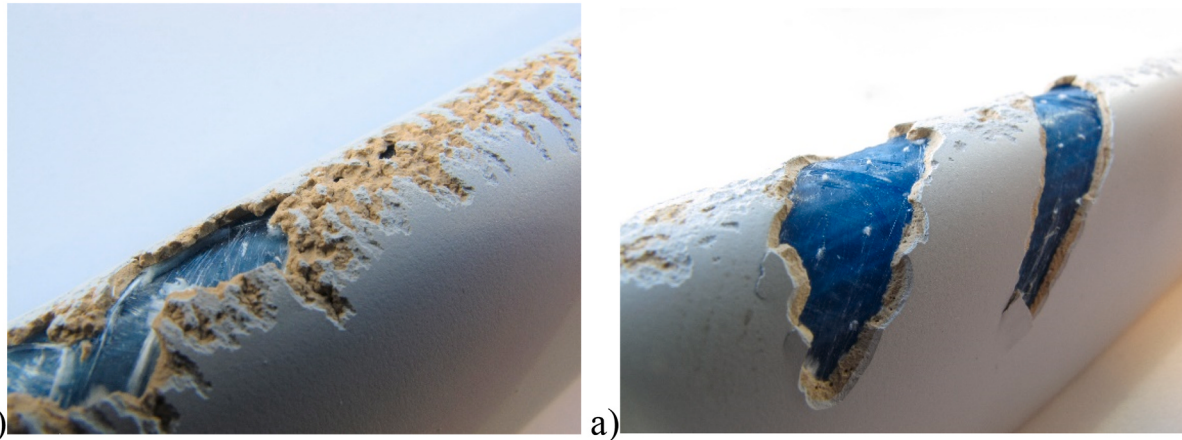


**Fig. 3.** Sections of RET specimens after testing: a) progressed erosion for 0.76 mm droplets, b) progressed erosion for 3.5 mm droplets.

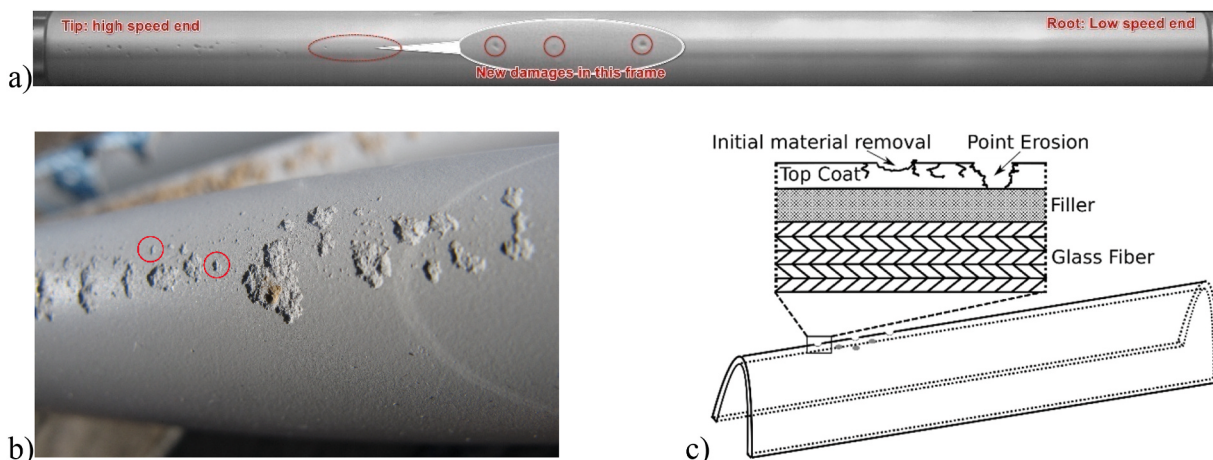


**Fig. 4.** a) RET specimen with initial damage points marked with circles, b) close up of initial damage points and further progressed erosion. c) schematic figure showing initial damage.

the impingement velocity  $v$  in bin  $i$ . Here  $v$  is the tip speed of a reference wind turbine according to the present wind speed, and  $n_i$  equals  $v$  multiplied by the relative liquid water content or number of droplets in the time bin.

The reference wind turbine is an IEA Wind 15 MW virtual offshore turbine with a hub height of 150 m, a rotor diameter of 240 m and a minimum tip speed of 63 m/s and a maximum tip speed of 95 m/s [14].

## 2.6. Meteorological data used for lifetime calculations

The meteorological data are 10-min observations of wind speed and precipitation from several meteorological stations. Data from nine stations in Denmark collected by the Danish Meteorological Institute (DMI), from seven stations in Germany collected by the German Weather Service (DWD) and from one station in Norway collected by the Norwegian Meteorological Institute (NMI) based on data from MET Norway are used. The data from these 17 stations are from rain gauges. Data from a research site in the UK collected by Natural Environment Research Council's Data Repository for Atmospheric Science and Earth Observation is used. The UK precipitation data is collected by disdrometer [18]. Further information about the data collection is provided in Ref. [19].

Only rain data are used for lifetime calculation, i.e. we omit solid precipitation (snow, hail). Snow is not expected to cause erosion. Hail is infrequent.

The data quality control and precipitation hydrometeor type filtering is presented in Ref. [6] for the Danish stations and in Ref. [20] for the UK station. The German and Norwegian data we assume are quality controlled by the data providers.

The duration of the time-series vary. The UK time series is 2.6 years long and the Norwegian time series is 3.3 years long. The Danish time series vary from 13.6 to 18.3 years and the German time series vary from 21.9 to 28.2 years. The wind speeds at all sites are observed at 10 m height except at three German sites: Grosser Arber and Seehausen at 15 m height and Arkona at 24 m height.

The wind speeds are extrapolated to 150 m using the power law wind profile with alpha = 0.143 according to Ref. [21].

## 3. Measures of impinging rain and effects of drop size on erosion damage

### 3.1. Representations of impinging rain

Rain erosion is commonly considered as a fatigue phenomenon. In classical fatigue theory, the load parameter is denoted  $S$  for stress, and  $N$  denotes the number of load cycles. A plot of sustained load cycles to failure as a function of applied stress is called an SN curve or Wöhler curve.

The simplest idealized rain field consists of spherical drops of equal diameter  $d$ , which are uniformly distributed in space. The volume concentration of water in the rain field,  $\psi$ , is calculated as follows:

$$\psi = \frac{I}{v_{drop, rp} * V_{drop}} \quad (4)$$

where  $I$  is the rain intensity and  $v_{drop, rp}$  is the fall velocity of the drops. The number of drops per  $m^3$ ,  $q$ , is

$$q = \frac{I}{v_{drop, rp} * V_{drop}} \quad (5)$$

$V_{drop} = (\pi/6)*d^3$  is the volume of one spherical drop with the nominal diameter  $d$ .

The rain field in a rain erosion tester is generated from an array of nozzles (needles) as described in the [13]. The rain field at the rotor plane can be quantified by its inner and outer diameters, the flow rate of water and the vertical distance from the nozzle array to the rotor plane.

When the test specimen travels through this rain field, the surface is exposed to repeated distributed impacts of the drops. For fatigue-based erosion modelling, it is practical to quantify the number of distributed repeated impacts causing stress cycles imposed on the surface. In Ref. [13] the number of impacts per unit area, denoted as specific impacts,  $N_A$ , is defined as:

$$N_A(t) = \frac{Pot}{2\pi(r_o - r_i)v_{drop, rp} * V_{drop}} = \frac{Pot}{2\pi(r_o - r_i)v_{drop, rp}} \cdot \frac{6}{\pi d^3} \quad (6)$$

with  $P$  being the flow of water entering the rain field,  $r_i$  and  $r_o$  are inner and outer radius of the rain field,  $\omega$  is angular velocity of the rotor, and  $t$  is the duration of rain erosion exposure. Here  $v_{drop, rp}$  is the fall velocity of the drops when entering the rotor plane.

[22] uses another parameter, also named specific impacts,  $N$ . It is the non-dimensional number of impacts per projected area of one droplet,  $(\pi/4)*d^2$ , where  $d$  is the nominal drop diameter. Using this definition and applying it to a RET as defined in Ref. [13],  $N_{ND}$  can be computed as

$$N_{ND}(t) = \frac{Pot}{2\pi(r_o - r_i)v_{drop, rp}} \cdot \frac{3}{2d} \quad (7)$$

[22] also defines the parameter, impingement,  $H$ . Impingement may be explained as the column of impacted water. Equivalent to precipitation measured on the ground, impingement is the quantity of rain measured by a virtual rain gauge, if it was mounted on the surface (blade leading edge), travelling through the rain field. Impingement  $H(t)$  is a function of the volume fraction of water in the atmosphere  $\psi$ , the relative impact velocity  $v$  and the time  $t$ .

$$H(t, r) = \psi * v(r) * t \quad (8)$$

Combining the impingement in a RET as described in Ref. [13] with the definition of impingement, we find, that  $H$  is equal to the specific impacts  $N_A$  ( $m^{-2}$ ) multiplied by the volume of one drop.

$$H(t) = \frac{Pot}{2\pi(r_o - r_i)v_{drop, rp}} \quad (9)$$

In the results section the RET data will be plotted for each of the three representations, Equations (6), (7) and (9).

### 3.2. Models for drop size dependency

Modelling of expected lifetime in the field requires knowledge of the effect of drop size on the damage rate, as natural rain contains a continuous range of drop sizes from a few micrometers up to approximately 6 mm. Testing a leading-edge protection (LEP) configuration with a range of drop sizes is expensive and time consuming. In the case, that test data is available for only one or a few drop sizes, models may be needed to predict VN curves for other drop sizes.

In the kinetic energy model proposed by Ref. [11] the assumption is that one universal fatigue curve having the kinetic energy of a drop relative to the impacted surface as the  $S$  parameter, and number of impacts per unit area as the  $N$  parameter, can be used across drop sizes.

$$N_A = cE_k^{-m} \quad (10)$$

$$N_A = c \left( \frac{1}{12} \pi \rho d^3 v^2 \right)^{-m} \quad (11)$$

$N_A$  is the number of impacts per unit area,  $E_k$  is the kinetic energy of the drop relative to the impacted surface.

[15] suggests an approach based on [10].

$$N_s(v, d) = \frac{8.9}{d^2} \cdot \left( \frac{S_{ec}/\gamma_m}{\gamma_f \cdot \bar{\sigma}_0} \right)^m \quad (12)$$

Where  $s_{ec}$  and  $\bar{\sigma}_0$  are both functions of the dynamic impedances of coating, substrate and liquid, and the ratio of drop diameter to coating

thickness ( $d/h_c$ ).  $\bar{v}_0$  is also a function of the impact speed. The two models of [10,11] do not take into account the  $m$  exponents dependency of the drop size.

### 3.3. New proposed models for drop size dependency

Here we propose two new models for the drop size dependency.

The first “equivalent impingement” assumption provides a quick and easy method to shift VN curves from one drop size to another. We assume, that the VH data fall on the same curve for any drop size, with  $H$  being the impingement. The impacts per unit area for one drop size can be converted into impacts per area for another drop size by multiplying by the ratio between the nominal drop volumes of the two sizes.

$$N_{d_2} = N_{d_1} \left( \frac{d_1}{d_2} \right)^3 \quad (13)$$

Earlier observations indicate a trend towards flatter VN curves with higher  $m$  and higher  $c$  values with decreasing drop size [23]. The present study supports this, as will be shown in the results section.

The second model is an empirical model, where the coefficient  $c$  and the exponent  $m$  from eq. (1) are functions of the drop size  $d$ .

$$H(d, v) = c(d)v^{-m(d)} \quad (14)$$

This method requires RET data for different drop sizes, and determination of functions for  $c(d)$  and  $m(d)$ . Fitting of parameters to experimental data is explained in Section 4.3.

## 4. Results

### 4.1. Drop size measurements

The rain fields in the RET was characterized applying a disdrometer.

The drop sizes and fall velocities from three of the four needle and flow rate configurations are presented in Fig. 5. Relative frequency curves are shown to the right and above of the coordinate system. The rain fields of G27 at 60 l/h (green dots) and G30 at 85 l/h (yellow dots) are relatively uniform with narrow distributions while the spray mode

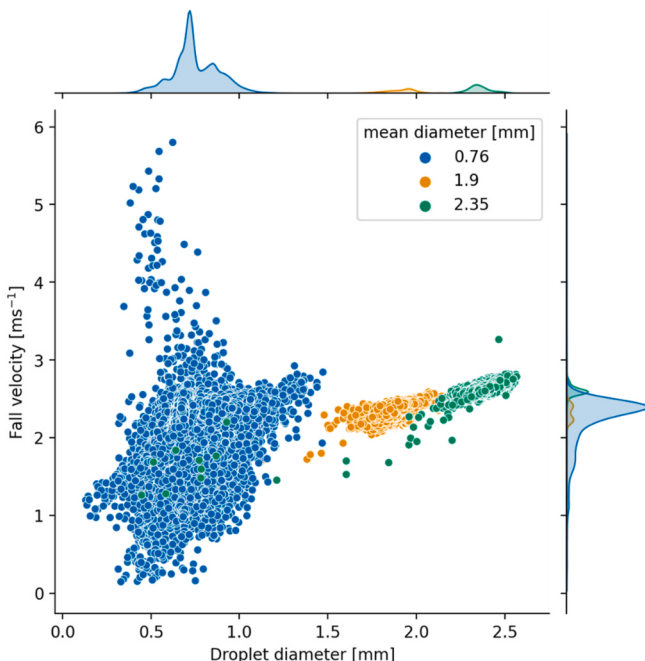


**Fig. 5.** Disdrometer observations of droplet size and fall velocity for G27 60 l/h (2.38 mm), G30 85 l/h (1.90 mm) and G27 105 l/h (0.76 mm) in RET at standstill. Distribution plots on the right and above.

G27 at 105 l/h (blue dots) shows a much broader distribution both in drop size and fall velocities. There is little overlap in droplet diameter for the different configurations. A few green dots of the G27 at 60 l/h rain field have much smaller diameter compared to the 2.35 mm average. They are a result of drops hitting the disdrometer housing and breaking up. These false values have been removed before calculating the mean values. All mean values and standard deviations are listed in Table 1.

Disdrometer observations were not available for G20 at 120 l/h standard flow rate. Drop count and volume measurements were done to determine the average drop size, and the relative variation is assumed to be similar to that of the G27 at 60 l/h configuration. The fall velocity was computed according to Refs. [13,16].

### 4.2. Rain erosion test results

Observations of end-of-incubation damage for each of four nozzle and flow configurations at three different rotor speeds, 800, 996 and 1193 rpm from RET are presented. The images captured during testing were analyzed manually as described in section 2.4 and [16]. The raw data are pairs of time and local velocity for each observed new erosion point. All the test data points are shown in Fig. 6. Note that the longest test durations here approach 100.000 s (28 h).

RET data are typically computed into representations, which are useful for lifetime predictions and correlations to field conditions, and for comparing test results performed at different test conditions. In the following, three such representations are shown: Specific impacts from Ref. [13] and specific impacts and impingement from Ref. [22]. For each representation, a power law function is fitted to the data according to Ref. [24]. Here velocity is considered as the dependent parameter, as the test is interrupted at a predetermined time, and the resulting velocities, at which damage occurred, are the results.

#### 4.2.1. Specific impacts - per area as in DNVGL-rp-0171

In [13,15] “specific impacts” denote the number of drop impacts per unit area of the surface. For the RET it is calculated from eq. (6). The plots in Fig. 7 show the velocity versus the number of impacts per square meter at end of incubation for the four drop sizes. For each drop size a power law function, eq. (1), is fitted to the data. These curves are known as VN<sub>A</sub> (Velocity-Number) curves. The exponent,  $m$  of the four VN<sub>A</sub> curves are shown in Table 2. The curves generally shift towards fewer impacts per square meter with increasing drop size by approximately two orders of magnitude from smallest to largest drop size. This is intuitively correct, since small drops impacting a surface supposedly affect a smaller area compared to larger drops.

#### 4.2.2. Specific impacts - non-dimensional as in ASTM G73

[22] uses a different definition of “specific impacts”. Here it is assumed that a drop impact on a surface affects an area equivalent to the projected area of the nominal drop diameter. Eq. (7) is used to calculate the specific impacts. The plots of the non-dimensional impacts data are shown in Fig. 8. The exponents of the fitted curves are similar to those of Fig. 5, but the curves are shifted closer together, because the number of impacts refer to the affected area.

#### 4.2.3. Impingement

Impingement, denoted as  $H$ , is another parameter used in Ref. [22]. In short it may be explained as the column of impacted water. Impingement is calculated as shown in Section 3.1, eq. (9). RET data converted to impact velocity versus impingement, is plotted in Fig. 9. These plots may be called VH curves.

The four VH curves intersect in the region around  $H = 2$  m and  $v = 125$  m/s, and the trend is higher  $m$  and higher  $c$  values of the VH curves with decreasing drop size.

The G27 - 105 l/h results with average drop size of 0.76 mm are slightly more aggressive than the 1.9 mm droplets. However, the spray

**Table 1**

Disdrometer measurements of droplet mean diameter and average fall velocity at the rotor plan in RET and standard deviations (std) for different needles and flow rates. For G20 disdrometer data were not available.\*Measured by drop count and volume. \*\*Calculated in accordance with [13]. \*\*\*estimated standard deviations.

Needle type	Flow rate (l/h)	Flow mode	Droplet diameter (mm)		Fall velocity (m/s)		Fall height (mm)
			Mean	Std	Mean	Std	
G20	120	Standard	3.50*	0.14***	2.12**	0.1***	280
G27	60	Standard	2.38	0.10	2.07	0.09	280
G30	85	Standard	1.90	0.11	2.32	0.11	400
G27	105	Spray	0.76	0.73	2.35	0.34	400

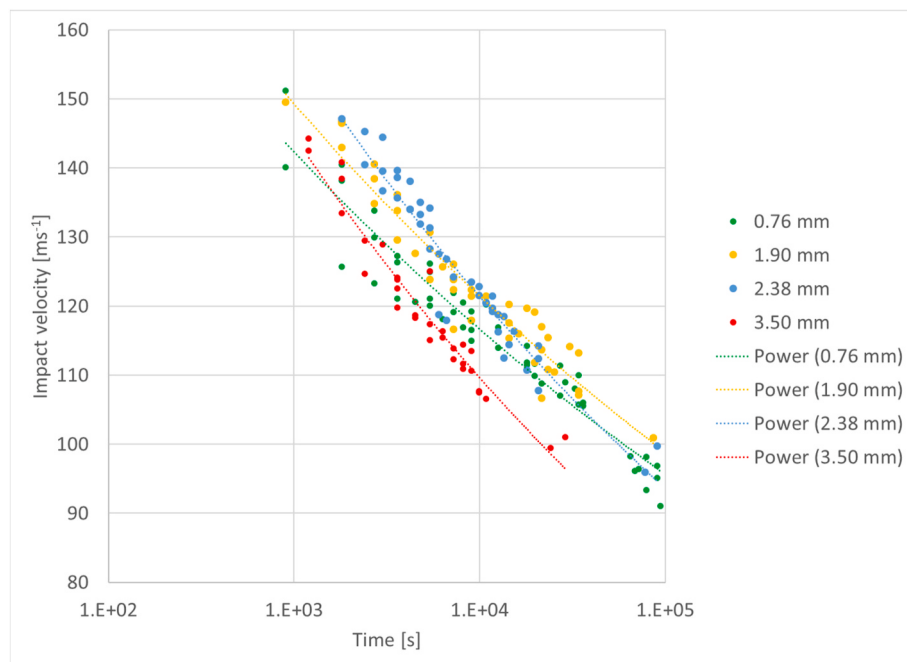


**Fig. 6.** Data points (time, velocity) for end of incubation of rain erosion tests conducted at four different nozzle-flow rate configurations.

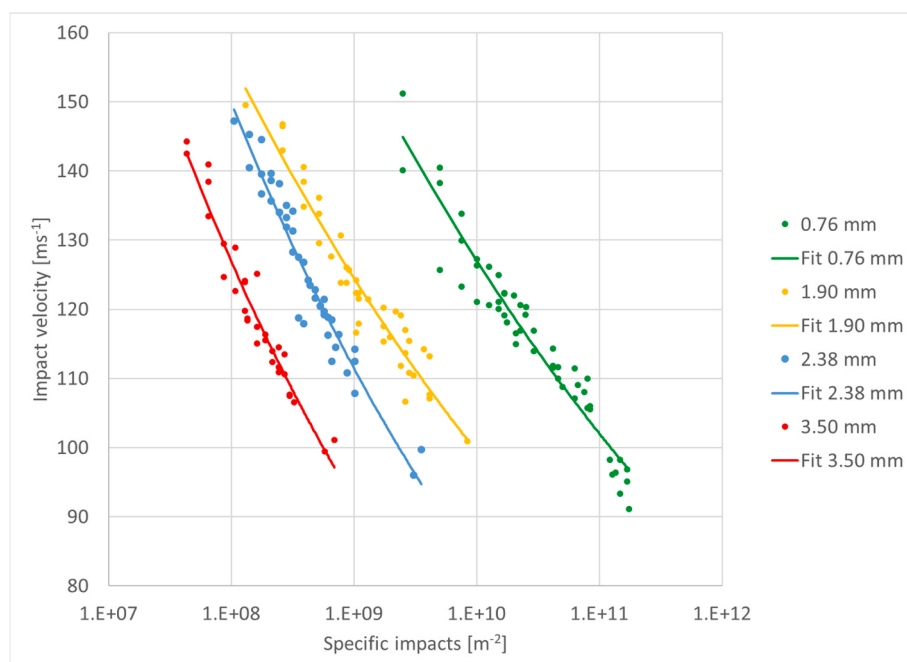


**Fig. 7.** Impact velocity versus specific impacts ( $\text{m}^{-2}$ ) at end of incubation.

**Table 2**

Power curve coefficients  $c$  and exponents  $m$  for four drop sizes when fitted to velocity versus impingement data for end of incubation.  $H_{100} = H(100 \text{ ms}^{-1})$ .

Needle gauge - Flow rate [l/h]	Droplet diameter [mm]	$c$	$m$	SD	$H_{100}$	95% confidence interval
				[m]		lower upper
G27-105	0.76	2.85E+22	10.5	0.82	28.2	23.9 34.4
G30-85	1.90	1.00E+22	10.2	0.96	34.1	26.9 46.1
G27-60	2.38	5.82E+16	7.8	0.64	16.4	13.8 20.3
G20-120	3.50	3.71E+15	7.2	0.68	12.6	10.9 15.2

mode setup, the G27 - 105 L/h, causes a large variation in drop sizes and falling velocities, so the 0.76 mm curve is more uncertain. The overlapping VH data points indicate, that impingement  $H$  is a governing parameter for erosion damage.

#### 4.3. Drop size dependency models

In this section the models from section 3.2 are used shifting the VNA data with 2.38 mm as the reference to 0.76, 1.90 and 3.50 mm drop sizes. The shifted curves are compared to experimental data for 0.76, 1.90 and 3.50 mm drops.

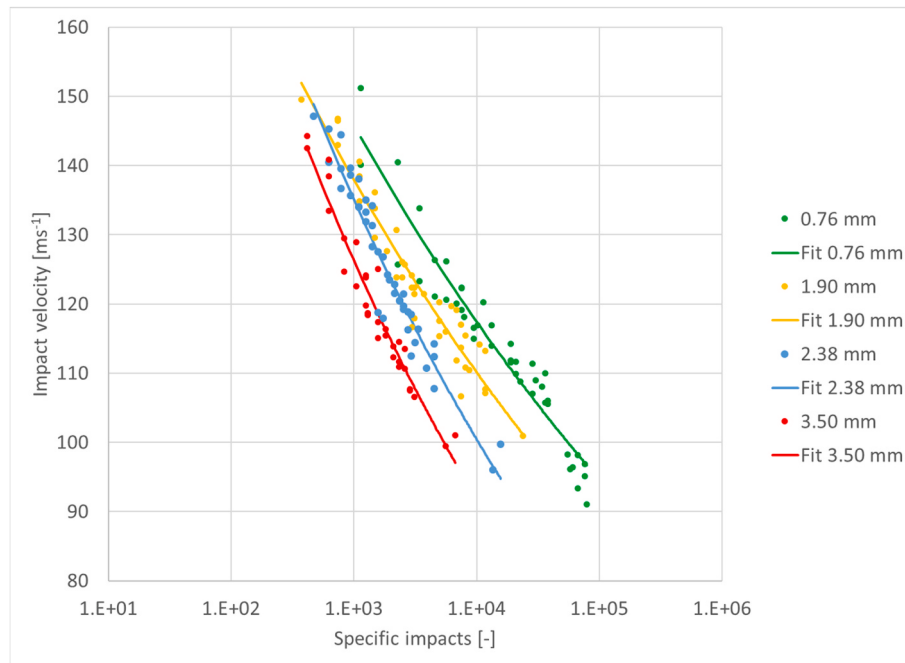


Fig. 8. Impact velocity versus specific impacts (non-dimensional).

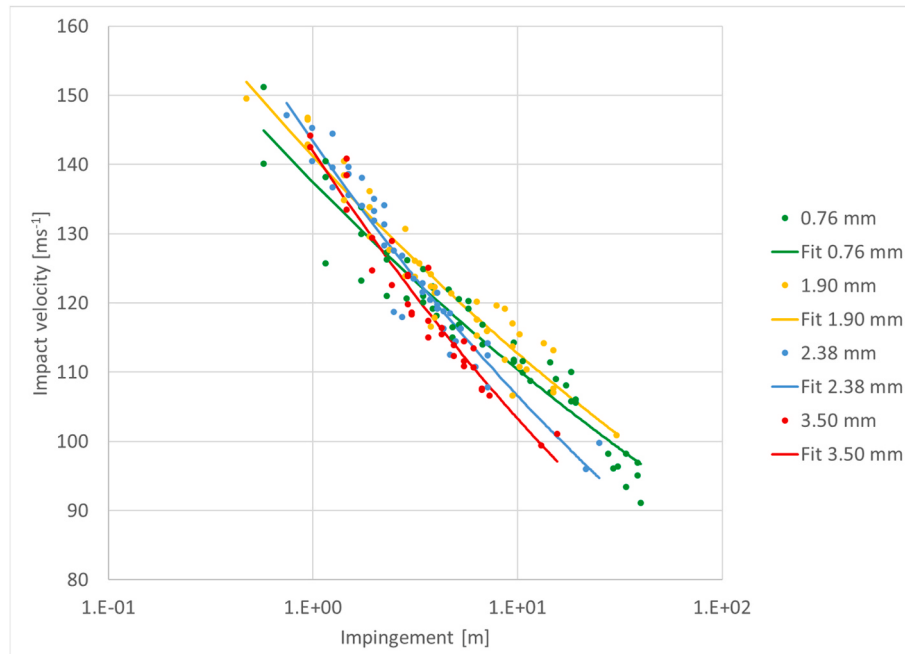


Fig. 9. Impingement versus impact velocity according to Ref. [22].

**Fig. 10** shows the 2.38 mm RET data shifted to other drop sizes using the kinetic energy model [11]. The resulting dotted curves are compared to the power law fits to experimental data. The kinetic energy model highly overestimates the effect of the drop size.

The methodology of [15] was applied for shifting the 2.38 mm data to the other drop sizes. The coating thickness is 150  $\mu\text{m}$ , and the thick putty is considered as the substrate. Guessed values of densities and speed of sound for both coating and putty are used.  $\rho_s = 1400 \text{ kg/m}^3$ ,  $c_s = 1200 \text{ m/s}$ ,  $\rho_c = 1100 \text{ kg/m}^3$ ,  $c_c = 700 \text{ m/s}$ . In this case the  $VN_A$  curves shifted to other drop sizes give a reasonable match to experimental data, see **Fig. 11**. However, the  $VN_A$  curves shifted to other drop sizes depend heavily on the chosen values of density and speed of sound of coating and substrate. Moreover, the slope of the curves does not vary with drop size.

Using the equivalent impingement assumption, eq. (13), the experimental curve for the 2.38 mm drops can be shifted to other drop sizes as shown in **Fig. 12**. The shifted curves also show reasonable matches with experimental curves, except for the slopes.

#### 4.4. Fitting the empirical drop size dependent impingement model $H(d)$

For realistic lifetime calculations of blade leading edges in the field it is necessary to take into account the effect of varying drop sizes. Here we present an empirical approach to determining drop size dependent parameters of VH curves as shown in Equation. 14. A sequence of (six) steps leads to establishing the functions  $c(d)$  and  $m(d)$ .

I. Data sets from RET with at least three different drop sizes are needed. Each data set is fitted to a power law, see Equation (1). The fitted  $c$  and  $m$  parameters for the experimental VH curves shown in **Fig. 9** can be seen in **Table 2**. Values of  $m$  are similar to those of **Figs. 7** and **8**.

II. The  $m$  values as function of drop size are plotted and fitted to a mathematic expression,  $m(d)$ . Here two functions are used. A linear function for simplicity, and a softsign function, which is a better fit to the data, see **Fig. 13**. The linear function is defined as

$$m(d)_{\text{linear}} = a_l d + b_l \quad (15)$$

where  $a_l$  is the scaling parameter, and  $b_l$  is shifting parameter.

The softsign function is defined as

$$m(d)_{\text{softsign}} = a_s \frac{d - d_0}{1 + |d - d_0|} + b_s \quad (16)$$

where  $a_s$  is a scaling parameter, and  $d_0$  and  $b_s$  are shifting parameters along the abscissa and ordinate respectively. The fitting is performed with non-linear least squares method.

III. The shifting parameter function,  $c(d)$ , of the drop size dependent power law, Equation (14), is chosen so it reflects the expected impingement to damage for the tested drop sizes, at 100  $\text{ms}^{-1}$  ( $H_{100}$ ), see **Fig. 9** and **Table 2**.  $H_{100} = c100^{-m}$  of the four VH curves are plotted in **Fig. 14**. 100  $\text{ms}^{-1}$  is chosen as a reference velocity, because it is within the range of measured data points, and it is relatively close to tip velocities of modern large turbines. The correlation of  $H_{100}(d)$  is also fitted to a linear function and a softsign function, shown in **Fig. 14**.

The shifting parameter  $c(d)$  in the drop size dependent power function is determined as

$$c(d) = H_{100}(d)100^{m(d)} \quad (17)$$

The fitted paremetres for the linear and the softsign models for  $m(d)$  and  $H_{100}(d)$  as functions of drop sizes are listed in **Table 3**.

Now  $m(d)$  and  $c(d)$  are parameterized, and the fatigue curve, Equation (14), can be plotted for any drop size. As we have two fits for  $m(d)$  and  $c(d)$ , the linear fit and softsign fit, we achieve two parametric models for drop size dependent impingement. The empirically determined drop size dependent erosion life model using softsign fits, Equation (14), and linear fits, Equation (15), are plotted with dashed lines for the four drop sizes tested in **Fig. 15 a) and b)** respectively. The experimental data fits are shown as solid lines. The model replicates the trend of the experimental data. The VH curves are more steep (smaller exponent,  $m$ ) for larger drop sizes, and the expected life at 100 m/s decreases with increasing drop size.

#### 4.5. Lifetime modeling

The average annual damage and expected average lifetime are computed as explained in sections 2.5 and 2.6 for different meteorological stations and applying different VH curves. **Fig. 16** shows the expected average lifetimes for the three Danish sites Billund, Anholt and

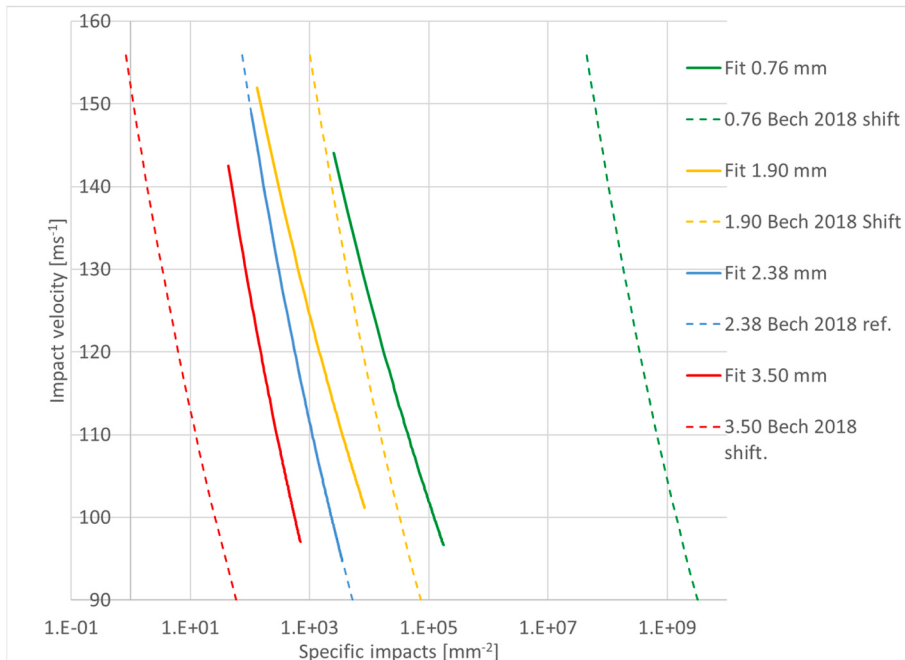


**Fig. 10.** The 2.38 mm data shifted to other drop sizes using the kinetic energy model [11] and fits to experimental data.

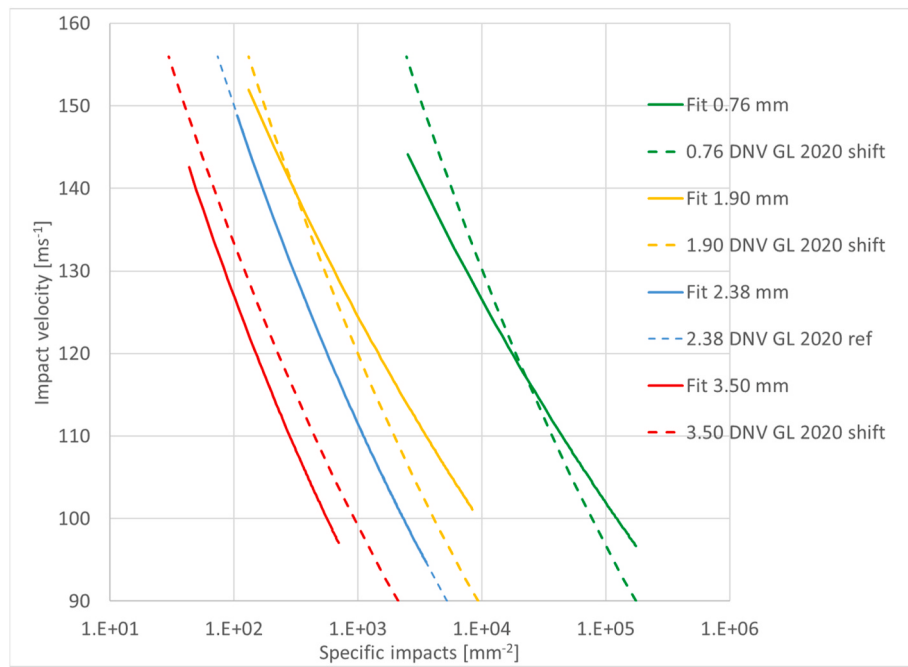


**Fig. 11.** Reference VN curve for 2.38 mm drop shifted to 0.76, 1.90 and 3.5 mm drops using method of [15]. Shifted curves are compared to fitted experimental curves for the other drop sizes.

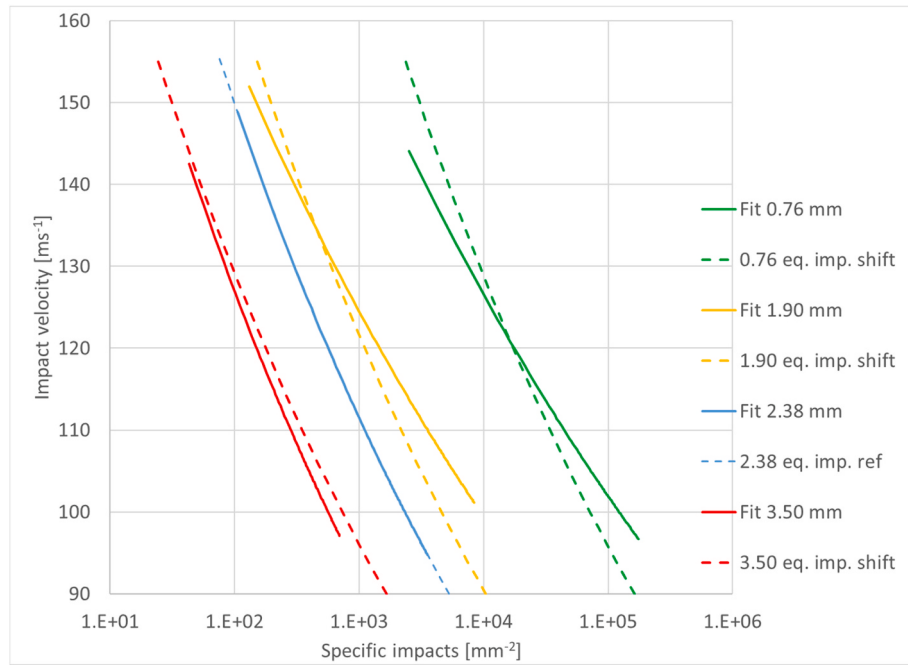


**Fig. 12.** Curves shifted using a proposed equivalent impingement assumption and compared to experimental fits.

Hvide Sande, computed using the individual VH curves of the four drop sizes tested, and the new drop size dependent VH(d) functions.

The VH curves of the larger drop sizes, the 2.38 mm and 3.50 mm have low exponents, and consequently give shorter lifetimes compared to the 0.76 mm and 1.90 mm drops. The drop size dependent softsign function predicts a lifetime very close to that of the 0.76 mm fixed curve. The softsign function gives less extreme  $m$  values for small and large droplets compared to the linear model. Consequently, the expected life time at the 18 sites analyzed is  $7\% \pm 0.6\%$  shorter when using the linear function compared to the softsign function.

**Fig. 17** shows the expected average lifetime for 18 sites predicted by applying the fixed parameter VH curve for 2.38 mm drops and for the drop size dependent fatigue function VH(d) with softsign parameter fitting. The predicted lifetimes range from 1.5 years (Utsira) to 10.8 years (Seehausen) for the fixed 2.38 mm VH curve and from 3.4 years (Utsira) to 25.5 years (Seehausen) for the softsign VH(d) function. On average the expected life when using the softsign fitted VH(d) function is 2.35 times longer than the lifetime predicted when using the 2.38 mm VH curve.

The annual precipitation varies more than a factor of two between

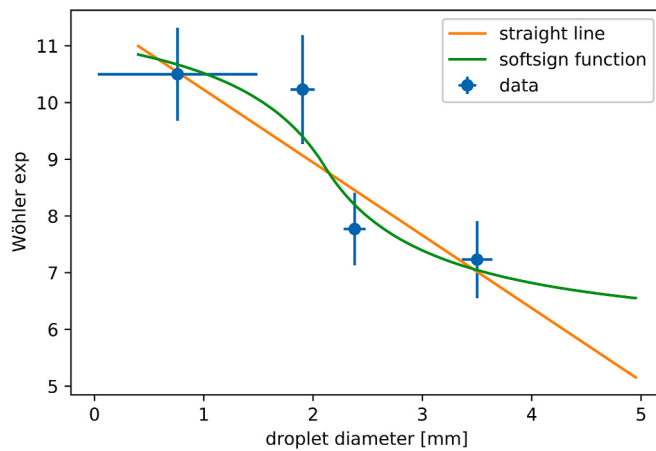


Fig. 13. The plot shows the exponents of the power law fits for the VH data of four average drop sizes.

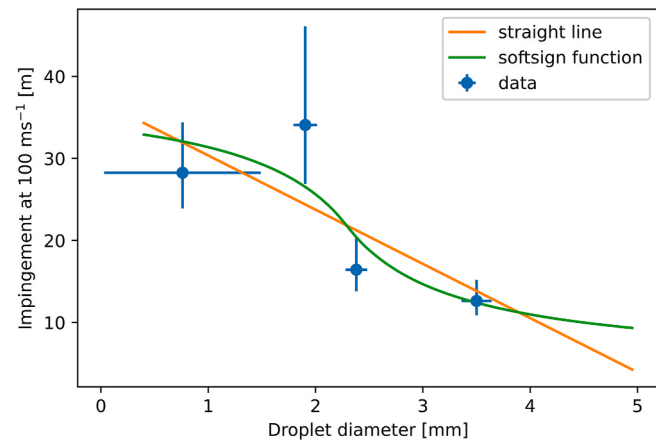


Fig. 14. The plot shows the expected average impingement to end of incubation at  $100 \text{ ms}^{-1}$  of the power law fits for the VH data of four average drop sizes.

Table 3  
Fitted parameters used in linear and softsign model for  $m(d)$  and  $H_{100}(d)$ .

Parameter	model type	coefficients		
		a	b	$d_0$
m	linear	11.7	-1.3	
	softsign	-3.1	8.9	2.1
$H_{100}$	linear	37.0	-6.6	
	softsign	-17.1	21.7	2.3

the 18 sites. This is however not the only source of the differing expected lifetimes. Fig. 18 shows a graphical representation of the accumulated damage per meter of precipitation for the 18 sites. These numbers vary from  $0.08 \text{ m}^{-1}$  at Seehausen to  $0.27 \text{ m}^{-1}$  at Utsira, when modelling by the softsign drop size dependent VH curves. The graphic shows a trend of higher damage per meter of precipitation for coastal and offshore sites compared to onshore sites. An exception is Grosser Arber, which is a windy mountain peak at nearly 1500 m altitude. The reason for the higher damage per precipitation is higher wind speeds concurrent with the rain events as described in Ref. [6].

## 5. Discussion

Some of the methods, results and assumptions are discussed in the

Results section. Additional assessment and considerations are given below.

### 5.1. RET results and representations of impinged rain

The non-dimensional specific impacts used in Ref. [22], may be considered equivalent to the number of load cycles sustained by a material element. This may be a useful parameter, when analyzing the mechanisms of fatigue in rain erosion. Specific impacts as defined in Ref. [13] is less useful, as it refers to the same surface area,  $\text{m}^2$  or  $\text{mm}^2$ , regardless of the drop size. Each drop impacts affects an area, which is somehow proportional to the size of the drop. Even a very high number of impacts with very small droplets on a given surface may cause little damage. In contrast, the number of specific impacts to failure may be less than one by this definition, if the drop diameter is large, and the reference area is small.

The impingement parameter, H, having meters as the unit, quantifies a virtual column of accumulated rain on the leading edge, regardless of the drop size. The RET data for different drop sizes overlap each other when the impacted rain is represented by the impingement. H may be considered as the governing factor driving rain erosion.

Impingement is also a useful measure, because it is easy to relate with key measures of wind turbines and meteorology. Thus, an upper bound of annual impingement can be estimated using the definition of impingement in Equation (7).

$$\text{max annual impingement} \approx \frac{\text{annual liquid precipitation}}{\text{average rain drop fall velocity}} * \text{rated tip velocity}$$

For example a turbine having a constant tip velocity of  $95 \text{ ms}^{-1}$  on a site with annual liquid precipitation of  $0.6 \text{ m}$ , assuming average fall velocity of  $6 \text{ ms}^{-1}$ , an upper bound of annual impingement can be estimated as  $(0.6\text{m}/6 \text{ ms}^{-1}) * 95 \text{ ms}^{-1} = 9.5 \text{ m}$ . The VH curve for 2.38 mm drops gives an average expected impingement life of  $24.5 \text{ m}$  at  $95 \text{ ms}^{-1}$ . A lower bound for expected life of this turbine is then  $24.5\text{m}/9.5 \text{ myr}^{-1} = 2.6 \text{ yrs}$ . The expected average life modelled using time series and the 2.38 mm VH curve is 2.8 yrs for Skagen and 5.0 yrs for Aalborg. Both sites have  $0.6 \text{ m}$  of annual precipitation.

### 5.2. Shifting RET curves tested at one drop size to other drop sizes

Different methods for shifting RET data from one drop size to other drop sizes are considered. The Kinetic Energy shift method from Ref. [11] highly overestimates the effect of drop sizes. Meaning that smaller droplets yield too little expected damage according to the model, whereas large drops yield too much damage. This method is applied in Ref. [19], where the exaggerated drop size dependency is reflected in an almost twice as large relative variation of expected lifetimes between the sites, compared to those computed in the present work. Here the value for Utsira is excluded, due to issues with this data set in Ref. [19]. The Kinetic Energy shift method was also applied in Ref. [6] for fewer stations, in Ref. [25] for one station and in Ref. [20] for one station, which has disdrometer drop size distribution data. In Ref. [20] the Kinetic Energy shift method gives unrealistic long expected life times for the data sets dominated by low rain intensities, where the Best model predicts very small droplets. The Drop Size Dependent Impingement model presented in this paper is expected to give better correlations with the expected life time modelled from actual measured drop sizes. The method of [15] and the simpler Equivalent Impingement method, presented here, give more realistic translations of the VN curves. However, they don't change the slopes of the curves as required according to the experimental observations. The present authors suggest to use VH curves and establish a correlation for the exponent  $m$  as function of the drop size  $d$ .  $m(d)$  can be fitted from RET data obtained with different drop sizes. The relatively large scatter of the RET data results in high uncertainty of a phenomenological  $m(d)$  correlation. Here we have

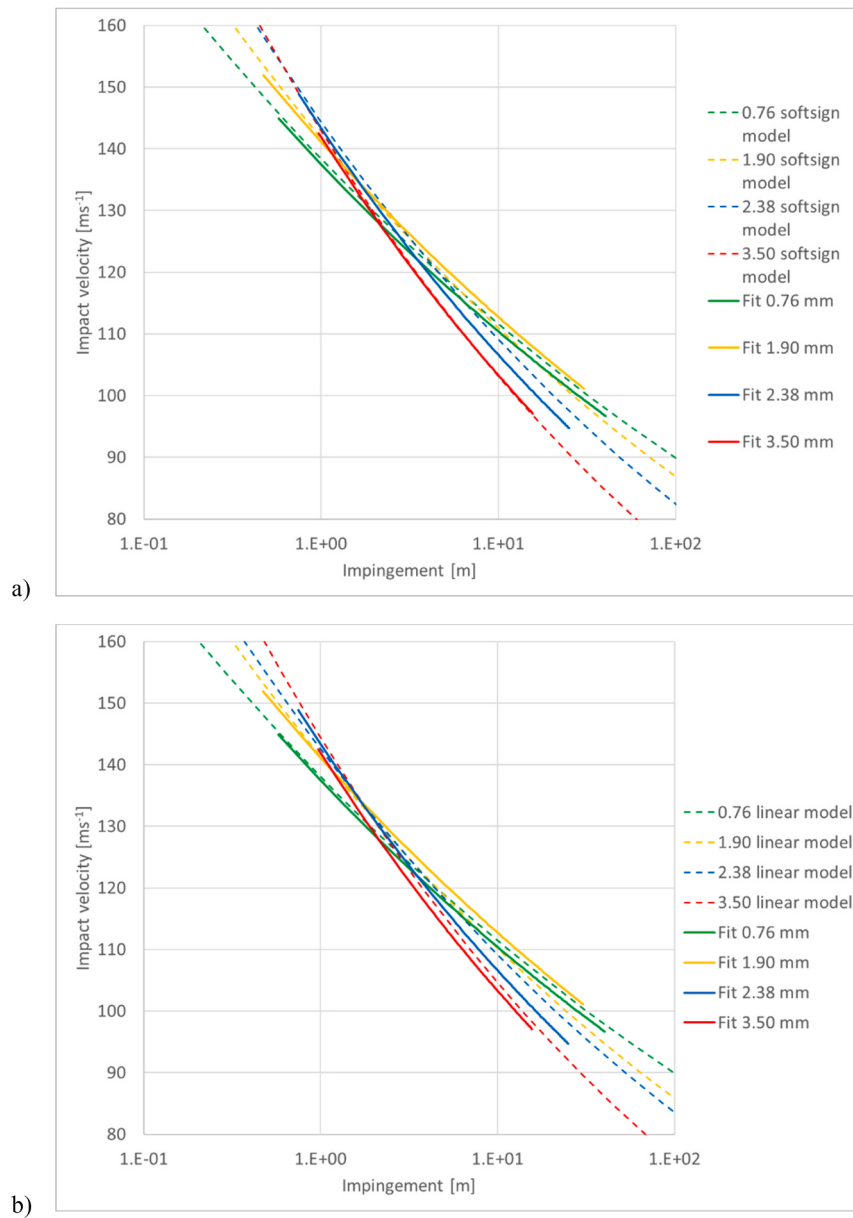


**Fig. 15.** The plot shows the VH curves for a range of drop sizes according to a) the softsign and b) the linear drop size dependent model.

proposed to fit to a linear and a softsign correlation. A logic next step would be a mechanistic approach to determine the type of correlation.

### 5.3. Lifetime modelling and drop size dependency

Looking at Fig. 17, the life times predicted when applying the drop size dependent VH(d) function are on average 2.35 times longer than those predicted by the fixed parameters VH curve for 2.38 mm drops. This reflects, that most of the observed rain rates imply smaller drop sizes than 2.38 mm, and the VH(d) curves for the smaller drop sizes are flatter and yield a smaller damage increment per meter of impinged rain at rotor impact velocities. If the method of the current governing recommended practice [15] is followed, we expect very conservative predicted lifetimes close to those of the fixed 2.38 mm VH curve, since that method does not imply a change of VN curve slope as function of drop size. The drop size dependent softsign function predicts a lifetime very close to that of the 0.76 mm fixed curve. It seems, the distribution of drop sizes in the spray mode corresponds somehow to the distribution of drop sizes coming from the measured rain intensities and the assumption

of Best d<sub>50</sub> drop sizes as function of rain intensity. This indicates, that the drop size distribution in the G27 – 105 l/min spray mode may correspond to the annual drop size distribution for rain in Northern Europe.

### 6. Limitations and proposals for further research

1. The present study does not account for other meteorological parameters like UV and temperature and the environmental degradation of coating properties over time. Research on how environmental degradation affects VH curves over time would enable more realistic lifetime predictions.
2. The Palmgren-Miner assumption for linear damage accumulation is not validated for rain erosion. We do not consider the effects of sequences of loading with differing drop sizes and impact velocities. This could be pursued by sequential block loading in rain erosion testing with different test conditions.
3. The lifetime predictions are not validated by field evidence from real turbines. It would be highly valuable for the wind industry and the research community, if rain erosion tests and models could be

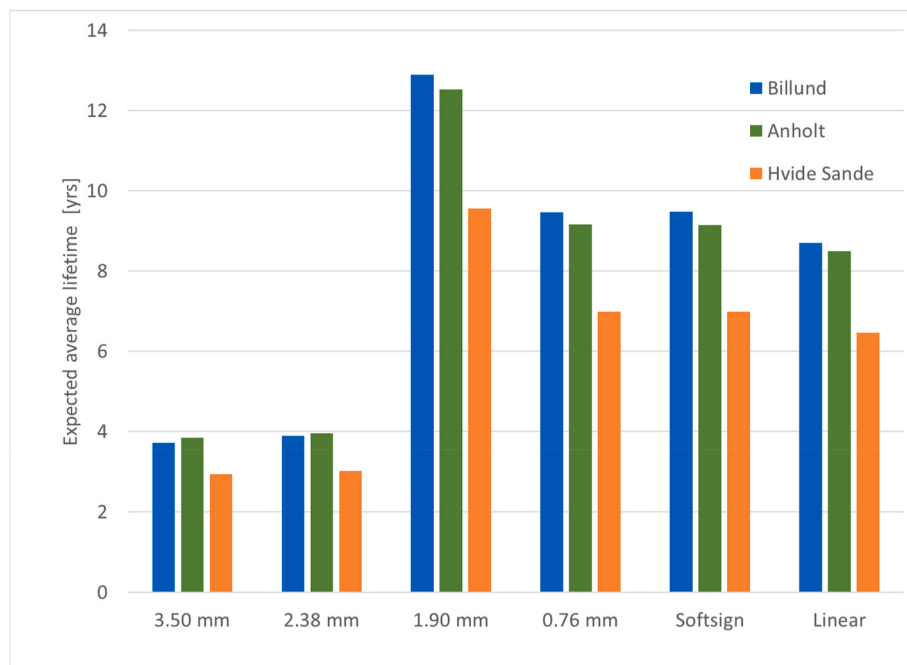


**Fig. 16.** Expected average lifetime, using the erosion model applied to the meteorological data from Billund, Anholt and Hvide Sande. Results are shown using the impingement model, based on each of the four different drop sizes independently, and for the two drops size dependent models, softsign and linear.

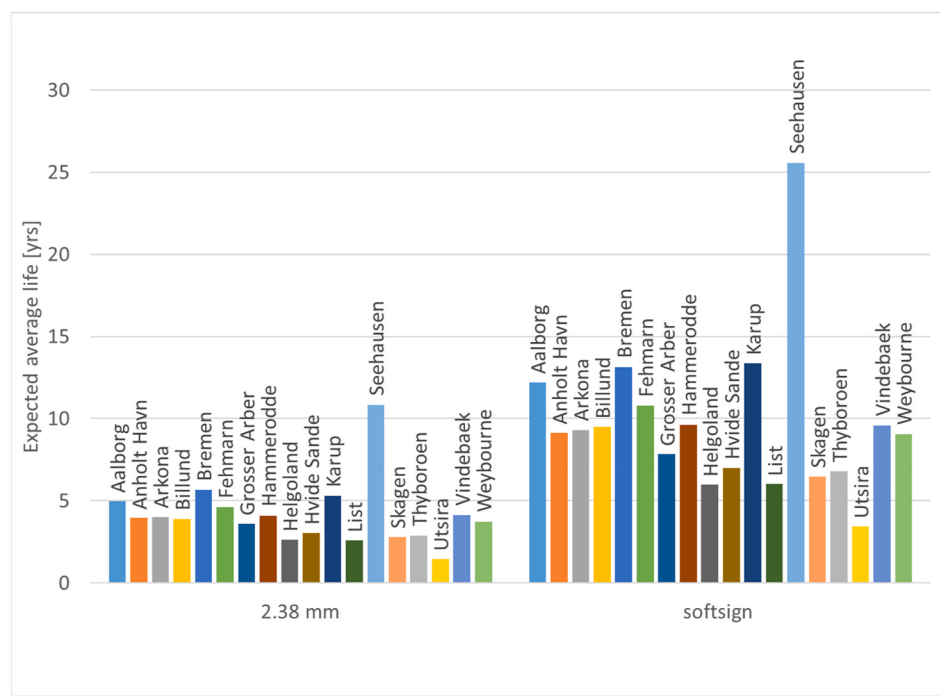


**Fig. 17.** Expected average lifetime for 18 different sites based on fixed parameter VH curve for 2.38 mm drops and for the drop size dependent fatigue function VH(d) with softsign parameter fitting.

- compared one-to-one with field observations through sharing of leading edge protection configurations and history of meteorological and operational conditions and observed erosion at operating wind farms.
- The correlations between drop size and erosion curves only relate to the specific coating configuration tested. The phenomenological empirical model for drop size dependency requires rain erosion tests with a number of different drop sizes, which is expensive and time consuming. Numerical models and assessment of material properties

from laboratory testing should be further developed, so rain erosion testing could be efficiently geared and supplemented by numerical exploration of the parameter fields.

- The drop sizes used for lifetime prediction are based on a simplified model, correlating rain intensity with an average drop size. In the atmosphere drop size distributions are not functions of rain intensity only. Further studies are needed to explore how drop size distributions vary with wind speed, shear and turbulence air pollution, temperature, humidity, altitude, and other local parameters.



**Fig. 18.** Average accumulated damage per meter of rain, computed from time series and using the softsign drop size dependent VH curves.

6. Hail and solid particles may also contribute significantly to leading edge erosion. Further research is needed on this topic.
7. The tests here are performed at velocities ranging from 90 to 150  $\text{ms}^{-1}$ , with test durations up to 27 h. The function fitted to the data are then extrapolated to the range of 60–95  $\text{ms}^{-1}$ . Further testing at lower velocities should clarify the validity of extrapolating VH curves.

## 7. Conclusion

The present experimental study focuses on the importance of the drop sizes in rain erosion testing of leading edge protection systems for wind turbine blades. Through rain erosion testing of a modern high performance top coat on glass fiber/epoxy specimens with four different rain fields, representing average drop sizes from 0.76 mm to 3.5 mm we demonstrate, that the slopes of the VN and VH curves decrease with decreasing drop size, corresponding to an increasing exponent of the fitted power law. We propose to use the Impacted Water Column, also named Impingement,  $H$  (meters), as the global measure for quantifying impinging rain on wind turbine blades, and in rain erosion testing, in favor of the Specific Impacts,  $N_A$  ( $\text{meters}^{-2}$ ), which is used in a current recommended practice. One argument is, that the VH curves for the drop sizes tested intersect (overlap) each other in the range of tested velocities, so that the incubation period in terms of impingement is in the range of 2–3 m at 128 m/s for all drop sizes tested. The decreasing slope with decreasing drop size gives, that the smaller drop sizes result in longer erosion life at lower velocities relevant for wind turbine rotors. The other argument is, that  $H$  is a practical measure in the sense, that it scales directly with precipitation as measured with a rain gauge multiplied by the ratio between the blade tip speed and the average fall velocity of the rain. Reading the  $H$  value at the relevant blade tip speed gives a direct indication of expected erosion life. In contrast  $VN_A$  curves are orders of magnitude apart, as the expected life depend strongly on the assumed drop size. Expected lifetime in the range of  $10^7$  to  $10^{12}$  impacts per square meters are not so easy to relate directly to common measures of precipitation and rotor tip speed.

For site specific lifetime prediction we propose an empirical damage accumulation model with drop size dependent VH curves. The average

predicted lifetimes when using the drop size dependent VH( $d$ ) function with varying slope is 2.35 times longer than the lifetimes predicted when using the 2.38 mm VH curve with a fixed slope.

## Author contributions

JIB created the research concept and research plan for the specimen testing, developed the empirical models together with NF-JJ and calculated the lifetimes. NF-JJ described and compared the standard recommended practice ASTM and DNV-GL methods for specific impact and did the visual inspection analysis of the RET results. MBM ensured the RET was performed and conducted and collected disdrometer measurements in the RET. ÁH implemented the droplet size impingement models in the python code for lifetime prediction, erosion-safe mode and profit calculation, updated the use of meteorological data in the code and introduced the softsign interpolation method. CBH coordinated the Erosion project and takes part in analysis and discussions. All contributed to writing of the paper.

## Data availability

The meteorological data used in this study are openly available in the Natural Environment Research Council's Data Repository for Atmospheric Science and Earth Observation (CEDA), the Danish Meteorological Institute's (DMI) Frie Data repository, the German Weather Service (DWD) Climate Data Center, and The Norwegian Meteorological Institute (NMI) based on data from MET Norway.

## Declaration of competing interest

The authors declare that they have no known competing financial interests or personal relationships that could have appeared to influence the work reported in this paper.

## Acknowledgements

This work was supported by the Innovation Fund Denmark - Grand Solutions projects, Grant 6154-00018B "EROSION" and grant 9067-00008B "Blade Defect Forecast". Meteorological data from the Open Data Server of Deutscher Wetterdienst, the Norwegian Meteorological Institute, the Meteorological data from Natural Environment Research Council and the Danish Meteorological Institute are acknowledged. We warmly thank Flemming Vejen for quality control and filtering of precipitation data at the DMI stations and Anna-Maria Tilg for quality control and filtering of the precipitation data at the UK station.

## References

- [1] R. Herring, K. Dyer, F. Martin, C. Ward, The increasing importance of leading edge erosion and a review of existing protection solutions, *Renew. Sustain. Energy Rev.* 115 (2019), 109382, <https://doi.org/10.1016/j.rser.2019.109382>.
- [2] L. Mishnaevsky, C.B. Hasager, C. Bak, A.M. Tilg, J.I. Bech, S. Doagou Rad, S. Faerster, Leading edge erosion of wind turbine blades: understanding, prevention and protection, *Renew. Energy* 169 (2021) 953–969, <https://doi.org/10.1016/j.renene.2021.01.044>.
- [3] C. Bak, A.M. Forsting, N.N. Sorensen, The influence of leading edge roughness, rotor control and wind climate on the loss in energy production, *J. Phys. Conf. Ser.* 1618 (2020), <https://doi.org/10.1088/1742-6596/1618/5/052050>.
- [4] F. Papi, F. Balduzzi, G. Ferrara, A. Bianchini, Uncertainty quantification on the effects of rain-induced erosion on annual energy production and performance of a Multi-MW wind turbine, *Renew. Energy* 165 (2021) 701–715, <https://doi.org/10.1016/j.renene.2020.11.071>.
- [5] L. Mishnaevsky, K. Thomsen, Costs of repair of wind turbine blades: influence of technology aspects, *Wind Energy* 23 (2020) 2247–2255, <https://doi.org/10.1002/we.2552>.
- [6] C. Hasager, F. Vejen, J.I. Bech, W.R. Skrzypinski, A.M. Tilg, M. Nielsen, Assessment of the rain and wind climate with focus on wind turbine blade leading edge erosion rate and expected lifetime in Danish Seas, *Renew. Energy* 149 (2020) 91–102, <https://doi.org/10.1016/j.renene.2019.12.043>.
- [7] A. Shankar Verma, Z. Jiang, Z. Ren, M. Caboni, H. Verhoef, H. van der Mijle-Meijer, S.G.P. Castro, J.J.E. Teuwen, A Probabilistic Long-Term Framework for Site-

- specific Erosion Analysis of Wind Turbine Blades: A Case Study of 31 Dutch Sites, *Wind Energy*, 2021, pp. 1–22, <https://doi.org/10.1002/we.2634>.
- [8] A.S. Verma, Z. Jiang, M. Caboni, H. Verhoeft, H. van der Mijle Meijer, S.G.P. Castro, J.J.E. Teuwen, A probabilistic rainfall model to estimate the leading-edge lifetime of wind turbine blade coating system, *Renew. Energy* 178 (2021) 1435–1455, <https://doi.org/10.1016/j.renene.2021.06.122>.
- [9] B. Amirzadeh, A. Louhghalam, M. Raessi, M. Tootkaboni, A computational framework for the analysis of rain-induced erosion in wind turbine blades, part II: drop impact-induced stresses and blade coating fatigue life, *J. Wind Eng. Ind. Aerod.* 163 (2017) 44–54, <https://doi.org/10.1016/j.jweia.2016.12.007>.
- [10] G.S. Springer, C.-I. Yang, P.S. Larsen, Analysis of rain erosion of coated materials, *J. Compos. Mater.* (1974), <https://doi.org/10.1177/002199837400800302>.
- [11] J.I. Bech, C.B. Hasager, C. Bak, Extending the life of wind turbine blade leading edges by reducing the tip speed during extreme precipitation events, *Wind Energy Sci.* 3 (2) (2018) 729–748, <https://doi.org/10.5194/wes-3-729-2018>.
- [12] D. Eisenberg, S. Laustsen, J. Stege, Leading edge protection lifetime prediction model creation and validation, *Wind Europe* (2016) 1–7, 2016, <https://windeurop.e.org/summit2016/conference/submit-an-abstract/pdf/615282322865.pdf>.
- [13] G.L. DNV, DNVGL-RP-0171 Edition February 2018 Testing of Rotor Blade Erosion Protection Systems, 2018.
- [14] E. Gaertner, J. Rinker, L. Sethuraman, B. Anderson, F. Zahle, G. Barter, IEA Wind TCP Task 37: Definition of the IEA 15 MW Offshore Reference Wind Turbine, 2020, pp. 1–44. <https://github.com/IEAWindTask37/IEA-15-240-RWT>.
- [15] G.L. DNV, DNVGL-RP-0573 - Evaluation of Erosion and Delamination for Leading Edge Protection Systems of Rotor Blades, 2020.
- [16] S. Fæster, N.F.J. Johansen, L. Mishnaevsky, Y. Kusano, J.I. Bech, M.B. Madsen, Rain Erosion of Wind Turbine Blades and the Effect of Air Bubbles in the Coatings, *Wind Energy*, 2021, pp. 1–12, <https://doi.org/10.1002/we.2617>.
- [17] H.M. Slot, E.R.M. Gelinck, C. Rentrop, E. Van der Heide, Leading edge erosion of coated wind turbine blades: review of coating life models, *Renew. Energy* 80 (2015) 837–848, <https://doi.org/10.1016/j.renene.2015.02.036>.
- [18] B.S. Pickering, R.R. Neely III, D. Harrison, Natural environment research Council, the disdrometer verification network (DiVeN): particle diameter and fall velocity measurements from a network of thies laser precipitation monitors around the UK (2017–2019), C. for E.D.A, Natural Environ. Res. Coun. Met Off. (2019), <https://doi.org/10.5285/602f11d9a2034dae9d0a7356f9aef45>.
- [19] C.B. Hasager, F. Vejen, W.R. Skrzypinski, A.M. Tilg, Rain erosion load and its effect on leading-edge lifetime and potential of erosion-safe mode at wind turbines in the north sea and baltic sea, *Energies* 14 (2021), <https://doi.org/10.3390/en14071959>.
- [20] A.-M. Tilg, W.R. Skrzypinski, Á. Hannesdóttir, C.B. Hasager, Effect of Drop-Size Parameterization and Rain Amount on Blade-Lifetime Calculations Considering Leading-Edge Erosion 5th, 25, *Wind Energy*, 2022, pp. 952–967. <https://doi.org/10.1002/we.2710>.
- [21] S.A. Hsu, E.A. Meindl, D.B. Gilhouse, Determining the power-law wind-profile exponent under near-neutral stability conditions at sea, *J. Appl. Meteorol. Climatol.* 33 (1994) 757–765, [https://doi.org/10.1175/1520-0450\(1994\)033<0757:DTPLWP>2.0.CO;2](https://doi.org/10.1175/1520-0450(1994)033<0757:DTPLWP>2.0.CO;2).
- [22] ASTM, G73-10, Standard Test Method for Liquid Impingement Erosion Using Rotating Apparatus, 2010, pp. 1–19, <https://doi.org/10.1520/G0073-10.2>. Astm. i.
- [23] N.F.-J. Johansen, Test Methods for Evaluating Rain Erosion Performance of Wind Turbine Blade Leading Edge Protection Systems, Ph.D. Thesis, Technical University of Denmark, 2020, <https://orbit.dtu.dk/en/publications/test-methods-for-evaluating-rain-erosion-performance-of-wind-turb>.
- [24] ASTM, E739 – 10: standard practice for statistical analysis of linear or linearized stress-life ((S-N) and strain-life ( $\epsilon$ -N) fatigue data, *Stat. Anal. Fatigue Data* 10 (2009), <https://doi.org/10.1520/stp29332s>, 129–129–9.
- [25] W.R. Skrzypinski, J.I. Bech, C.B. Hasager, A.M. Tilg, C. Bak, F. Vejen, Optimization of the erosion-safe operation of the IEA wind 15 MW reference wind turbine, *J. Phys. Conf. Ser.* 1618 (2020), <https://doi.org/10.1088/1742-6596/1618/5/052034>.